Journal of Pharmaceutical Analysis 12 (2022) 791–800

Contents lists available at ScienceDirect

Journal of Pharmaceutical Analysis

journal homepage: www.elsevier.com/locate/jpa

Original article

Effective extraction of fluoroquinolones from water using facile modified plant fibers

Nan Zhang [a], Yan Gao [a], Kangjia Sheng [a], Wanghui Jing [a, b], Xianliang Xu [a], Tao Bao [a, b, *], Sicen Wang [a, c, **]

[a] School of Pharmacy, Xi'an Jiaotong University Health Science Center, Xi'an, 710061, China
[b] Institute of Chinese Medical Sciences, State Key Laboratory of Quality Research in Chinese Medicine, University of Macau, Macao, 999078, China
[c] Shaanxi Engineering Research Center of Cardiovascular Drugs Screening & Analysis, Xi'an, 710061, China

ARTICLE INFO

Article history:
Received 2 January 2022
Received in revised form
7 June 2022
Accepted 10 June 2022
Available online 14 June 2022

Keywords:
Fluoroquinolones
Cattail fiber
Carboxylation modification
In-syringe solid phase extraction

ABSTRACT

In this study, ecofriendly and economic carboxy-terminated plant fibers (PFs) were used as adsorbents for the effective in-syringe solid phase extraction (IS-SPE) of fluoroquinolone (FQ) residues from water. Based on the thermal esterification and etherification reaction of cellulose hydroxy with citric acid (CA) and sodium chloroacetate in aqueous solutions, carboxy groups grafted onto cotton, cattail, and corncob fibers were fabricated. Compared with carboxy-terminated corncob and cotton, CA-modified cattail with more carboxy groups showed excellent adsorption capacity for FQs. The modified cattail fibers were reproducible and reusable with relative standard deviations of 3.2%–4.2% within 10 cycles of adsorption-desorption. A good extraction efficiency of 71.3%–80.9% was achieved after optimizing the extraction condition. Based on carboxylated cattail, IS-SPE coupled with ultra-performance liquid chromatography with a photodiode array detector was conducted to analyze FQs in environmental water samples. High sensitivity with limit of detections of 0.08–0.25 μg/L and good accuracy with recoveries of 83.8%–111.7% were obtained. Overall, the simple and environment-friendly modified waste PFs have potential applications in the effective extraction and detection of FQs in natural waters.

1. Introduction

Fluoroquinolones (FQs), a type of broad-spectrum bactericides that inhibit DNA synthesis, are commonly used for the treatment of human and livestock pathogenic infections [1–3]. However, only a few FQs can be metabolized by organisms, and more than 70% of FQs are excreted into the environment in the form of prototypes [4]. FQ residues exhibit strong resistance to degradation because of the high chemical stability of C–F bonds. The discharge and long-term exposure to antibiotics can lead to drug resistance and environmental toxicity [5–8]. FQs have been identified as pharmaceuticals and personal care products pollutants. The European Union and North America have banned the use of ciprofloxacin (CIP) in aquaculture. The use of pefloxacin, ofloxacin, lomefloxacin (LOM), and norfloxacin has been prohibited in animal breeding [1,9]. Some reports have detected FQ residues in sewage sludge, hospital wastewater, and surface water [10]. Therefore, it is essential and pressing to monitor and remove FQ residues in natural waters to protect the health of living beings and ensure environmental safety.

Effective adsorbents are required for the enrichment and separation of targets prior to instrumental analysis due to low concentrations of FQs and matrix interference. Adsorbents also play an indispensable role in FQs removal. The adsorption method is more economical and feasible than oxidation, photocatalysis degradation, and membrane filtration in removing FQs [11–14]. Currently, metal organic frameworks (MOFs) [15], covalent organic frameworks (COFs) [16,17], molecularly imprinted polymers (MIPs) [18], and carbon-based materials [10] have been used for the adsorption of FQ pollutants from the aquatic environment. For example, Zhou and co-workers [19] prepared ionic liquid (IL)-COOH/Fe_3O_4@Zr-MOFs for the selective detection and adsorption of FQs. First, Fe_3O_4 nanoparticles were synthesized and modified using dopamine to provide sites for UiO-67 growth. Then, IL-COOH was introduced into Fe_3O_4@Zr-MOFs. Jiang et al. [16] prepared zwitterionic COFs through the solvothermal

Peer review under responsibility of Xi'an Jiaotong University.
* Corresponding author. School of Pharmacy, Xi'an Jiaotong University Health Science Center, Xi'an, 710061, China.
** Corresponding author. School of Pharmacy, Xi'an Jiaotong University Health Science Center, Xi'an, 710061, China.
E-mail addresses: baotao@xjtu.edu.cn (T. Bao), wangsc@mail.xjtu.edu.cn (S. Wang).

https://doi.org/10.1016/j.jpha.2022.06.004

method at 120 °C for 72 h and used the COFs to remove FQs. Tan et al. [20] synthesized MIP-coated mesoporous carbon nanoparticles through a series of chemical reactions consisting of Stöber synthesis, vinyl-functionalization, and polymerization to remove FQs from water. The developed materials exhibited good adsorption characteristics for FQs, but the synthesis of adsorbents involves multi-step reactions, expensive raw materials, and polluting organic solvents. To meet the high demand for environmental applications of waste from biomass resources, it is urgent to explore economical, environmental-friendly, and feasible methods to fabricate adsorbents based on waste fiber resource for the adsorption of FQs.

Plant fibers (PFs), such as corn stalk, cotton, and wood, are derived from biomass and have gained great interest for the adsorption of pollutants in the ecosystem due to their biodegradability, high specific surface area, sustainability, and abundant modified hydroxy group content [21–23]. Native PFs exhibit weak adsorption capacity, which is merely based on the interaction of hydroxy with the target compound. Surface modification was carried out to synthesize functionalized cellulose fibers to enhance their adsorption capacity [24]. Surface modification involves grafting functional groups on the surface of PFs through a series of chemical reactions, such as sulfonation, phosphorylation, polymer grafting, carboxylation, and carboxymethylation [21,25,26]. Carboxy groups can be efficiently introduced to PFs using carboxylation and carboxymethylation methods. Notably, compared with 2,2,6,6-tetramethylpiperidine-1-oxyl selective oxidation [27] and succinic anhydride esterification using pyridine [28], two simple, feasible, and green methods have been reported for random carboxy modification in aqueous solution based on the esterification between the hydroxy of PFs and citric acid (CA) [29], as well as on the etherification of hydroxy and sodium chloroacetate ($ClCH_2COONa$) [30]. Currently, carboxylated wood [31] and bamboo fibers [32] prepared using the hydrothermal method are used for adsorbing tetracycline and lead (II). Carboxymethylated wood fibers are also used for removing Cu^{2+} [33,34]. It is necessary to explore the variety of carboxy-modified PFs and more applications for waste resources.

Here, two methods based on CA and $ClCH_2COONa$ were implemented for the carboxy modification of PFs (Scheme 1). Carboxylated PFs were prepared by thermochemical esterification of PFs–OH with citric anhydride induced by CA. Carboxymethylated PFs were obtained after alkalization, etherification, and acidification of PFs. The readily-available and cellulose-rich cotton, corncob, and cattail fibers were chosen to be functionalized as potential adsorbents. Corncob and cattail are normally discarded or burned, causing environmental pollution. Using such waste resources for potential applications in environmental remediation is of great significance. According to the possible hydrogen bondings (–N–H···O and –O–H···O), Lewis acid-base (PF–COOH to piperazine ring), and electrostatic interactions between FQs and the modified fibers [10], the synthesized materials were packed in plastic needle tips for extraction and removal of FQs. Chemical information on the FQs is shown in Fig. S1. The carboxylated cattail was comparable with a commercial cation exchange resin in the adsorption of FQs. The applicability of the synthesized adsorbent was evaluated by using it to extract FQs from river water, wetland water, and pond water. The environment-friendly modified fibers are expected to be utilized in the extraction of FQs in natural water.

2. Experimental

2.1. Chemicals and materials

Enoxacin sesquihydrate (ENO), levofloxacin (LVFX), CIP, gatifloxacin (GAT), LOM, sulfamethazine (SMT), and ibuprofen (IBU) were bought from Yuanye Biotechnology Co., Ltd. (Shanghai, China). Bisphenol A (BPA) was obtained from Macklin Biotechnology Co., Ltd. (Shanghai, China). Anhydrous CA and $ClCH_2COONa$ were purchased from Aladdin Chemistry Co., Ltd. (Shanghai, China). High performance liquid chromatography (HPLC) grade trimethylamine, formic acid, phosphoric acid (H_3PO_4), sodium hydroxide (NaOH), hydrochloric acid (HCl), and acetic acid were bought from Kermel Chemical Reagent Co., Ltd. (Tianjin, China). Phenolphthalein was supplied by Tianxin Fine Chemical Development Center (Tianjin, China). HPLC grade methanol (MeOH) and acetonitrile (ACN) were obtained from Prochrom Technology Co., Ltd. (Beijing, China) and Fisher Scientific Co., Ltd. (Waltham, MA, USA), respectively. The 723 cation exchange resin was purchased from Jingbo Biotechnology Co., Ltd. (Xi'an, China). Ultrapure water was produced by a SIM-T10UV system from Fly Science Co., Ltd. (Beijing, China). Corncob, cattail, and cotton were supplied by Huashaoying Town (Hebei, China), Boxing County (Shandong, China), and Yangxue Sanitary Material Factory (Heze, China), respectively. The river water, wetland water, and pond water were collected from the Wei River (Xianyang, China), the Xin Wei Sha Wetland Park (Xianyang, China), and a pond in the Western China Science and Technology Innovation Harbor (Xianyang, China).

2.2. Instrumentation and chromatographic conditions

Field emission scanning electron microscopy (FESEM) analysis was studied by a MAIA3 LMH scanning electron microscope (Waltham, MA, USA). X-ray photoelectron spectroscopy (XPS) was performed on an ESCALAB 250Xi spectrometer (Thermo Fisher Scientific Inc., Waltham, MA, USA) using a monochromatized Al Kα source ($h\nu$ = 1486.6 eV). Element analysis for C, H, N, and O was determined using a Euro EA3000 analyzer (Milan, Italy). Fourier transform infrared spectroscopy (FT-IR) spectra were recorded using a Bruker VERTEX70 spectrometer (Waltham, MA, USA). Analytes quantification was carried out on a Shimadzu LC 2040C 3D ultra-high performance liquid chromatography (UPLC) system (Tokyo, Japan) with a photodiode array (PDA) detector and 40 μL of the sample loop. The separation was carried out using a C_{18} column (75 mm × 2.0 mm i.d.) with a 2.2 μm particle size from Shimadzu (Tokyo, Japan) at 30 °C. The mobile phase consisted of (A) 25 mM H_3PO_4 aqueous solution (pH was adjusted to 3.0 with trimethylamine) and (B) ACN. The gradient program was as follows: 0–9 min, 10.5%–14% B; 9–10 min, 14%–10.5% B; and 10–13 min, 10.5% B. The flow rate was maintained at 0.3 mL/min. The wavelength number was set as 278 nm and the injection volume was 10 μL.

2.3. Synthesis of modified cotton, corncob, and cattail

2.3.1. Activation of PFs

Five grams of cotton was put in 400 mL of 0.1 M NaOH while stirring for 2 h to remove hemicellulose and inorganic composites. After washing with 300 mL of ultrapure water thrice, the cotton was immersed in 400 mL of 0.1 M HCl while stirred for 30 min to remove residual NaOH and neutralize CFs–ONa. The pretreated cotton was again washed with 300 mL of ultrapure water thrice and was dried at 60 °C. Corncob and cattail were smashed and were sieved through a 24-mesh (850 ± 29 μm) and a 50-mesh sieve (355 ± 13 μm) to obtain a 355–850 μm particle size. Ten gram of corncob particles was treated with 150 mL of 0.1 M NaOH while stirring for 2 h. After washing with ultrapure water thrice, the corncob was put into 150 mL of 0.1 M HCl while stirring for 30 min. Then, the corncob was washed with ultrapure water and dried at 80 °C. Ten g of sieved cattail was successively immersed in 250 mL of 0.1 M NaOH and 0.1 M HCl while stirring for 2 h and 30 min,

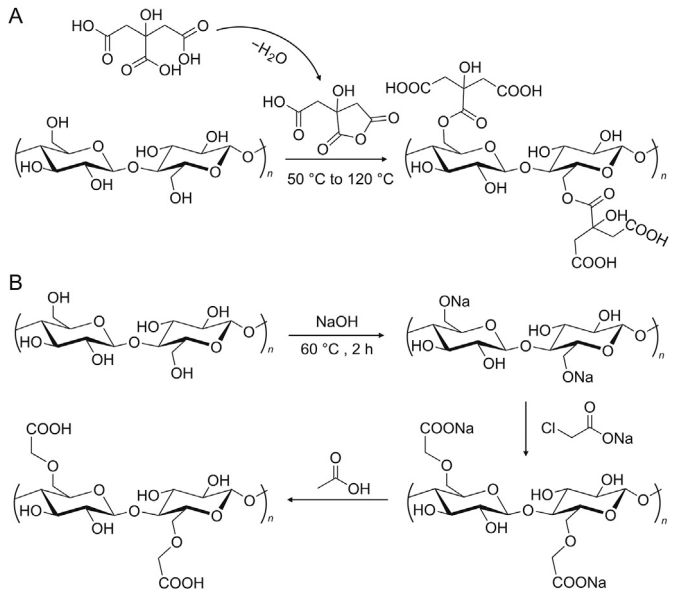

Scheme 1. Scheme of the (A) carboxylation and (B) carboxymethylation processes.

respectively. It was then washed thrice with 300 mL of ultrapure water and dried at 60 °C.

2.3.2. Carboxymethylation of PFs

Based on the alkalization, etherification, and acidification of PFs, carboxymethyl groups were grafted onto the PFs. Briefly, 0.8 g each of activated cotton, corncob, and cattail were added into 40 mL of 0.1 M $ClCH_2COONa$ with 5% NaOH and were reacted for 2 h at 60 °C [35]. The residues obtained were washed successively with 60 mL of 2 g/L acetic acid and ultrapure water and dried at 60 °C.

2.3.3. Carboxylation of PFs

Activated cotton (1 g), corncob (4 g), and cattail (2.5 g) were soaked in 50 mL of 0.5 M CA. The reaction system was kept at 50 °C for 24 h to form citric anhydride. After that, the temperature was raised to 120 °C for 90 min [36]. The carboxy groups were grown on the PFs through the thermochemical esterification of PFs–OH with citric anhydride. After washing with ultrapure water and drying at 60 °C, carboxylated cotton, corncob, and cattail were obtained.

2.4. Contents of carboxy groups

The carboxy contents of activated PFs, carboxylated PFs, and carboxymethylated PFs were determined by titration. Briefly, 0.25 g of fiber was put in 30 mL of 0.01 M NaOH stirring for 1 h. Then, 10 mL of the filtrate was titrated against 0.01 M HCl with phenolphthalein as indicator. The carboxy concentration of the fiber was calculated according to Eq. (1).

$$c_{COOH} = \left[\frac{(c_{NaOH} \times V_{NaOH}) - 3(c_{HCl} \times V_{HCl})}{m}\right] \quad (1)$$

where c_{COOH} (mmol/g) is the concentration of the fiber (mmol/g), and m (g) is the mass of fiber. c_{NaOH} and c_{HCl} (mol/L) are the concentrations of NaOH and HCl, respectively. V_{NaOH} (mL) is the volume of the NaOH solution and V_{HCl} (mL) is the volume of HCl solution used to titrate the sample.

2.5. In-syringe solid phase extraction (IS-SPE) procedure

The activated, carboxymethylated, and carboxylated PFs were synthesized for the extraction of FQs. 15 mg of each was packed in a cone-shaped plastic needle hub attached to a 20 mL syringe. The packed adsorbents were preconditioned using 7.5 mL of MeOH and 40 mL of ultrapure water at a flow rate of 1 mL/min by a syringe pump. A total of 10 mL of the sample solution at pH 7 containing the analytes was continuously pushed through the needle hub using a syringe pump at a flow rate of 1 mL/min. Then, 400 μL of the desorption solvent with 1% formic acid:ACN (9:1, *V*/*V*) was used to desorb FQs at a flow rate of 120 μL/min. A total of 10 μL of the eluent was injected into the UPLC system for analysis.

2.6. Determination of breakthrough for FQs

The breakthrough of the FQs was determined to investigate the removal performance of the adsorbent. A small amount of the adsorbent (15 mg) was packed in the plastic needle hub. Then, the aqueous sample solution with 40.5 μg/L ENO, 49.5 μg/L LVFX, 41.4 μg/L GAT, 40 μg/L CIP, and 54.6 μg/L LOM was loaded through the micro-column at a flow rate of 1 mL/min using a syringe pump. A 200 μL of outlet sample was collected at 6 min intervals and 10 μL of the solution was analyzed using the UPLC system. The loading was stopped when the outlet sample had the same concentration as the sample solution of FQs. The ratio of the outlet concentration (c_t) to the initial concentration (c_0) versus time was plotted to obtain the breakthrough curve. The points at $c_t/c_0 = 10\%$ and $c_t/c_0 = 90\%$ were referred to as the "point of breakthrough" and the "point of exhaustion," respectively. The amount of FQs adsorbed by the adsorbent (q, μg/g) was calculated according to Eq. (2) [37].

$$q = \frac{uc_0}{m}\int_0^{t_e}\left(1 - \frac{c_t}{c_0}\right)dt \quad (2)$$

where u (mL/min) is the flow rate, t_e (min) is the exhaustion time, and m (mg) is the mass of the adsorbent.

2.7. Sample preparation of the real samples prior SPE

The collected water samples, 250 mL each of river water, wetland water, and pond water, were slowly passed through the column (30 cm × 4 cm i.d.) packed with 30 g of 723 cation exchange resin (10 cm in height). Activation of the cation exchange resin is provided in the Supplementary data. The three water samples were adjusted to pH 7.0 using 10 M NaOH and were filtered through a 0.45-μm polyethersulfone (PES) membrane.

3. Results and discussion

3.1. Characterization

The morphology of the PFs was characterized using FESEM and the results are shown in Fig. 1. The surface of cotton was smooth and no impurities were observed before or after modification (Figs. 1A–C). Figs. 1D–F shows that carboxymethylated and carboxylated cattail had almost the same appearance as unmodified cattail. Abundant stripes and ravines were observed on the surface of cattail fibers, which is beneficial for grafting functional groups. The surface of corncob (Fig. 1G) was also rough with widespread folds, whereas the folds on carboxymethylated and carboxylated corncob (Figs. 1H and I) became round and raised. This could be due to the corncob getting swollen with NaOH solution during the activation process, leading to the surface of the corncob being raised and thicker.

The functional groups on the fibers were identified using FT-IR. The FT-IR spectra of unmodified, carboxymethylated, and carboxylated fibers shown in Fig. 2A appear to display similar patterns. The cotton, corncob, and cattail consisted of cellulose, hemicellulose, lignin, extractives, and ash [38–41] (Table S1). Accordingly, after the modification, the characteristic carboxy bands overlapped with their own adsorption peaks. The common adsorption bands at 3338, 1726, 1249, and 1033 cm^{-1} indicated the existence of cellulose, hemicellulose, and lignin [42]. The bands appearing at 3338 and 1033 cm^{-1} were ascribed to the stretching vibration of −O−H and −C−O−C− on the cellulose molecular chain, respectively. The bands at 1726 and 1249 cm^{-1} were assigned to the stretching vibration of −C═O and −C−O of the carboxylic groups [43], respectively. After modification, the bands at 1726 and 1249 cm^{-1} of corncob increased slightly, whereas they increased significantly on cattail and cotton, indicating that the carboxy groups were grafted on the fibers.

The crystalline structure of the fibers before and after modification was investigated using X-ray diffraction (Fig. 2B). The crystalline index (CI) was calculated using Eq. (3) [44].

$$\mathrm{CI}\ (\%) = \frac{I_{200} - I_{\mathrm{am}}}{I_{200}} \tag{3}$$

where, I_{200} and I_{am} are the intensities of the crystalline structure at 22.0° and the amorphous region at 19°, respectively. As shown in Fig. 2B, the common peaks at 14.5°, 16.7°, around 22° (22.5° for cattail and corncob, and 22.8° for cotton), and 34.5° for cotton and corncob correspond to planes 101, 110, 200, and 004 of cellulose I. After functionalization, the tiny peaks for cellulose II at 12.0° and 20.0° on carboxymethylated cotton were observed and corresponded to planes 110 and 210 [45], respectively. The transformation from cellulose I to cellulose II might have been caused by the high concentration of NaOH used in carboxymethylation. The intensity of the CI of modified cotton, corncob, and cattail fibers decreased (Table S2). The reduction in the number of hydrogen bonds was attributed to esterification and etherification of hydroxy groups led to less crystallization [28].

The elemental composition and chemical states were confirmed through element analysis and XPS analysis. Results are shown in Table S3 and Fig. 3. The peaks in the full-scan spectrum of carboxylated cattail were assigned to O1s, N1s, and C1s (Fig. 3A), whereas the minor peak corresponding to F1s was observed after the adsorption of FQs (inset of Fig. 3A). The high-resolution spectrum of C1s could be deconvoluted into three peaks assigned to C−C (284.8 eV), C−O (286.3 eV), and C═O (288.1 eV) (Fig. 3B). The high-resolution spectrum of N1s could be split into N−H (400.0 eV) and C−N (401.5 eV) [46] (Fig. 3C). After adsorption, no obvious shift in the binding energies was observed in the C1s and N1s spectra. The O1s spectrum could be separated into C−O (531.4 eV) and C═O (532.8 eV). With the adsorption of FQs, the binding energies of C−O and C═O shifted to 531.0 and 532.5 eV (Fig. 3D), respectively, which might have been caused by the existence of hydrogen bonds between FQs and the adsorbent.

3.2. Contents of carboxy groups

Cotton, cattail, and corncob are mainly composed of cellulose, hemicellulose, and lignin. According to the thermal esterification and etherification reactions between the cellulose hydroxy and CA/$ClCH_2COONa$, carboxy groups were grafted onto the surface of cotton, corncob, and cattail. The contents of the carboxy groups were identified using titration. The amounts of carboxy in carboxylated and carboxymethylated cotton were 0.651 and 0.473 mmol/g, respectively. The amounts of carboxy in carboxylated and carboxymethylated corncob were 0.759 and 0.627 mmol/g, respectively. The carboxylated and carboxymethylated cattail contained 0.906 and 0.848 mmol/g of carboxy, respectively. The amount of carboxy on the fibers grafted by CA (carboxylation) was larger than on the fibers grafted by $ClCH_2COONa$ (carboxymethylation), indicating that modification using CA was more efficient for grafting

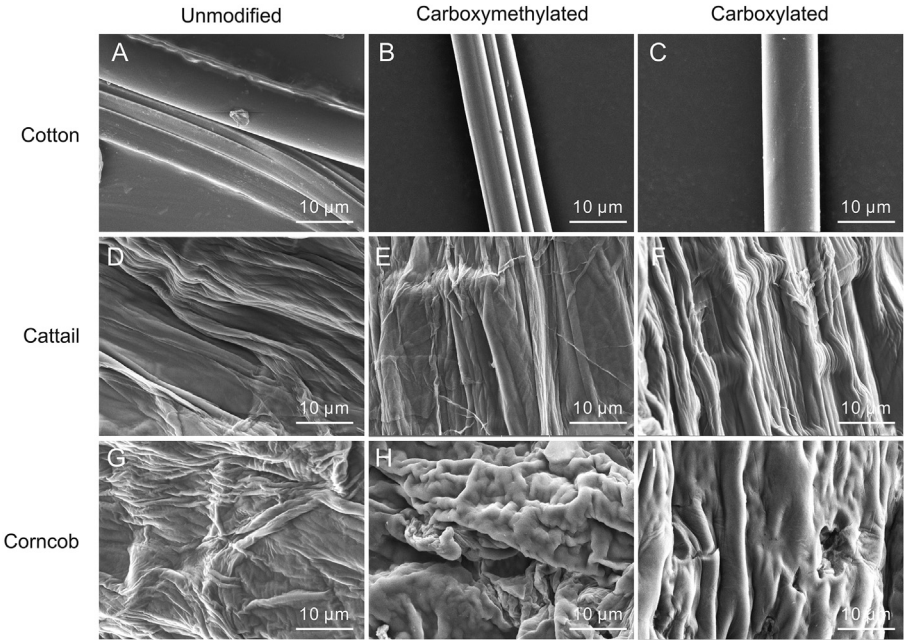

Fig. 1. Field emission scanning electron microscopy (FESEM) images at 10 μm of unmodified (A) cotton, (D) cattail, and (G) corncob; carboxymethylated (B) cotton, (E) cattail, and (H) corncob; and carboxylated (C) cotton, (F) cattail, and (I) corncob.

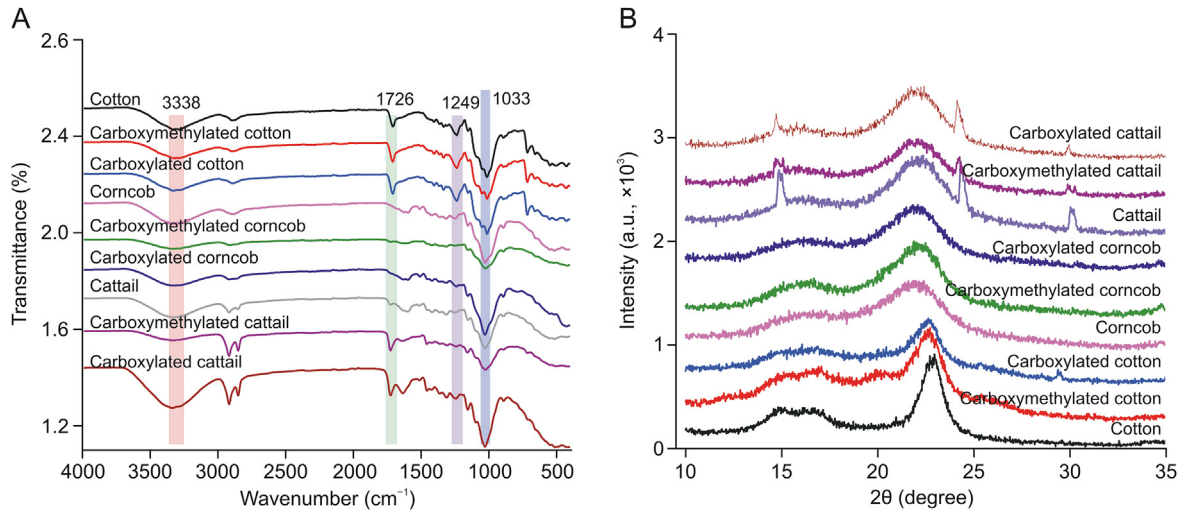

Fig. 2. (A) Fourier transform infrared (FT-IR) spectra and (B) X-ray diffraction patterns of unmodified, carboxymethylated, and carboxylated cotton, cattail, and corncob.

carboxy groups. After carboxylation, cattail with a high content of hemicellulose and lignin had the highest carboxyl content. Corncob and cattail exhibited higher carboxy grafting than cotton, which could be attributed to their rough surface and abundance of hydroxy groups that provided more grafting sites.

3.3. Extraction study of FQs

A total of 10 mL of the aqueous sample solution with 40.5 μg/L ENO, 49.5 μg/L LVFX, 41.4 μg/L GAT, 40 μg/L CIP, and 54.6 μg/L LOM was loaded to investigate the extraction performance of FQs using modified PFs. To enhance extraction capacity, different modified fibers were evaluated. Moreover, various factors affecting extraction efficiency, such as adsorbent amount, sample solution flow rate, pH, desorption solvent, eluent volume, and eluent flow rate, were investigated.

3.3.1. Screening of adsorbents

The activated, carboxymethylated, and carboxylated cotton, corncob, and cattail fibers were used for IS-SPE of FQs. Fig. 4 shows that the extraction efficiency (EE, %) of carboxylated fibers was greater than that of carboxymethylated fibers, whereas the EE of carboxymethylated fibers exceeded that of activated fibers. The higher content of carboxy in fibers grafted using CA enhanced the hydrogen bonding effect, leading to better EE. The extraction capacities of the activated fibers were found in the descending order of cattail > corncob > cotton, which could be attributed to the unique structure of the fibers. The high hemicellulose and lignin content of cattail provided stronger hydrogen bonding and van der Waals interactions. Considering superior extraction capacity, the carboxylated cattail was used as the optimal adsorbent for the extraction of FQs.

3.3.2. Optimization of IS-SPE procedure

The effect of the adsorbent (carboxylated cattail) amount on the extraction capacity (represented by the peak area) varying from 5 to 25 mg was investigated. As shown in Fig. 5A, the extraction capacity increased sharply when the amount of carboxylated cattail increased from 5 to 10 mg, whereas the extraction capacity increased slightly within the range of 10–25 mg. Therefore, 10 mg of carboxylated cattail was almost enough for IS-SPE of FQs in the sampling. 15 mg was used for the following extraction based on the comprehensive consideration of the EE and adsorbent amount.

The flow rate of the sample solution has an effect on the mass transfer of analytes in extraction. A low flow rate will consume extraction time while a high flow rate will save extraction time but can cause partial targets to flow out directly without contact with the adsorbent. The effect of sampling flow rate ranging from 0.5 to 2.5 mL/min is shown in Fig. 5B. The extraction capacity remained almost constant when the flow rate of the sample increased from 0.5 to 1 mL/min. Extraction capacity decreased continuously with the increase of the flow rate. Therefore, the sampling flow rate was set at 1.0 mL/min.

The pH, which affects the charge distribution of the adsorbent and the state of targets, has a major influence on the extraction performance. Acid compounds dissociate in anionic form when pH > pKa and exist in neutral or cation state at pH < pKa. However, the relationship between the charge state of basic compounds and pH is opposite to that of acidic compounds. FQs, as amphoteric compounds, consist of two ionizable functional groups, the carboxylic group (pK_{a1} 5.0–6.4) and the amino group of the piperazine moiety (pK_{a2} 7.6–9.0) [1,19] (Fig. S1). As shown in Fig. 5C, the optimal extraction capacity was obtained at pH 7. Most FQ molecules were zwitterionic at pH 7, and carboxylated cattail was neutral or negatively charged. Therefore, the Lewis acid-base interaction between FQs and the adsorbent was enhanced. The extraction capacity increased within the range of pH 4–7. FQs changed from cation/neutral to anion form and the adsorbent changed from cation to neutral, leading to the decrease of electrostatic repulsion. Both the adsorbent and the FQs were negatively charged when pH > 7, which increased the electrostatic repulsion. Hence, the pH of the sample solution was adjusted to 7.

After extraction, desorption solvents were screened to elute the analytes. ACN:water (1:9, *V*/*V*) with different proportions of formic acid was investigated to desorb FQs. Formic acid was added to destroy the electrostatic interaction between FQs and carboxylated cattail. As shown in Fig. 5D, as formic acid content increased from 0% to 1.5%, the extraction capacity increased and then remained constant. Therefore, ACN:1.0% formic acid aqueous solution (1:9, *V*/*V*) was chosen to desorb FQs in the desorption.

The effect of eluent volume on extraction capacity ranging from 100 to 500 μL was investigated. As shown in Fig. 5E, the total amount of FQs in the sampling was certain. As the eluent volume increased, the amount of targets per unit eluent decreased gradually, leading to the decrease of extraction capacity. High sensitivity

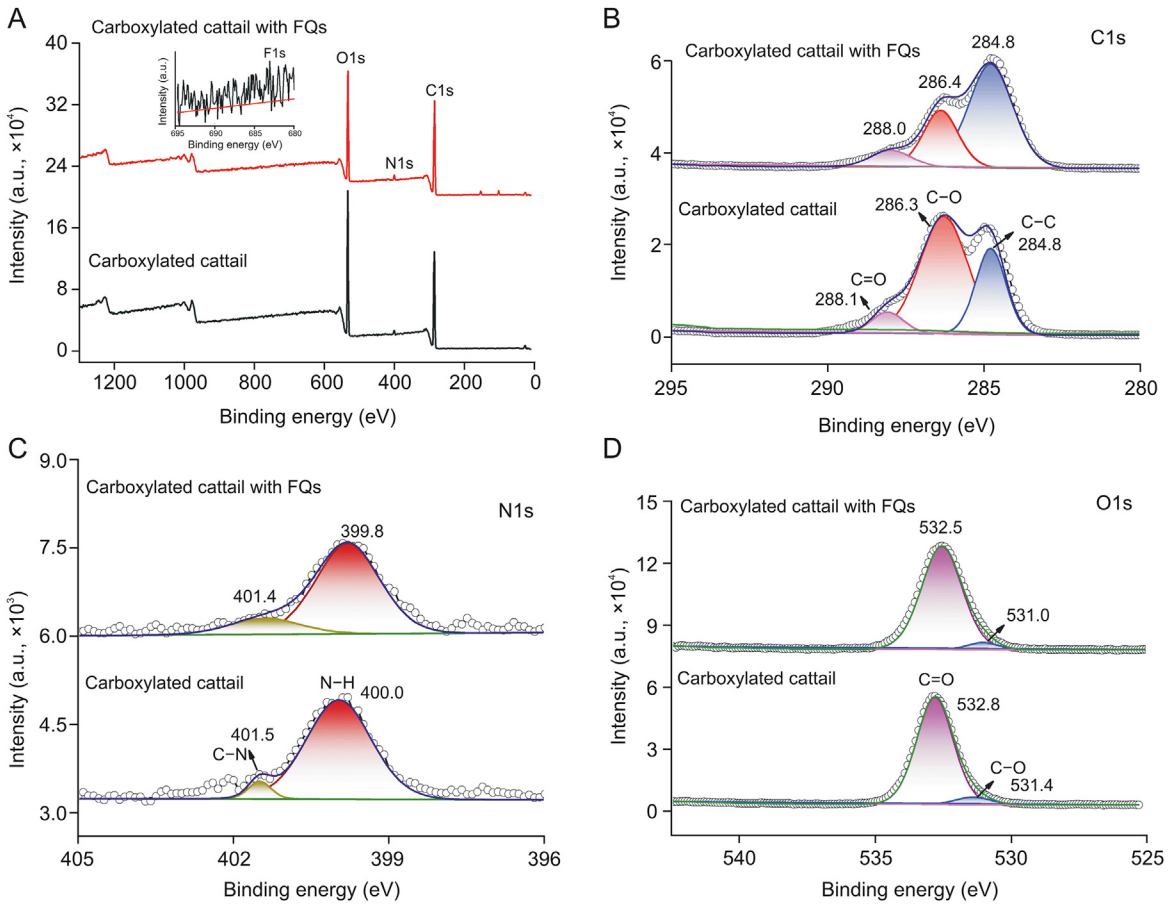

Fig. 3. Full-scan X-ray photoelectron (XPS) spectra of (A) carboxylated cattail and carboxylated cattail with fluoroquinones (FQs) (inset: the partial enlargement of full scan X-ray spectrum (695–680 eV)), and high-resolution spectra of (B) C1s, (C) N1s, and (D) O1s before and after adsorption.

was obtained with small volume eluents, which could cause incomplete desorption. Conversely, a large volume would make desorption complete but reduce the sensitivity. Therefore, considering the total extraction amount and sensitivity of FQs, 400 μL was used to desorb FQs in subsequent experiments. After elution, repeated desorption was conducted to investigate the residual amount of FQs on the carboxylated cattail. FQs in the second eluent were less than the limit of detection (LOD) (Fig. S2), indicating that desorption was adequate.

The eluent flow rate affected the mass transfer in the desorption of FQs, which was similar to the sampling flow rate. Fig. 5F shows that no obvious change was observed in the extraction capacity when the eluent flow rate increased from 40 to 120 μL/min. The variation of eluent flow rate had hardly any effect on the extraction capacity. To shorten the extraction time, a flow rate of 120 μL/min was chosen to elute FQs in the desorption process.

3.3.3. Adsorption selectivity

To verify the selective performance of carboxylated cattail, the adsorptions of SMT, LVFX, IBU, and BPA onto carboxylated cattail were tested. The adsorption conditions and analytical methods for adsorbing SMT, BPA, and IBU are illustrated in the Supplementary Data. As shown in Fig. S3, BPA with hydroxy group and IBU with carboxylic group were not adsorbed by the carboxylated cattail, and only a small amount of SMT (2.2% of EE) that contained amino and sulfonamide groups and a pyrimidine ring was adsorbed. However, the adsorbent showed excellent adsorption capacity for LVFX (84.8% of EE) that contained quinolone and piperazine moieties. Adsorption depends on the intermolecular interactions between the adsorbent and the target species. The low adsorption capacity could be ascribed to the weak intermolecular interactions between

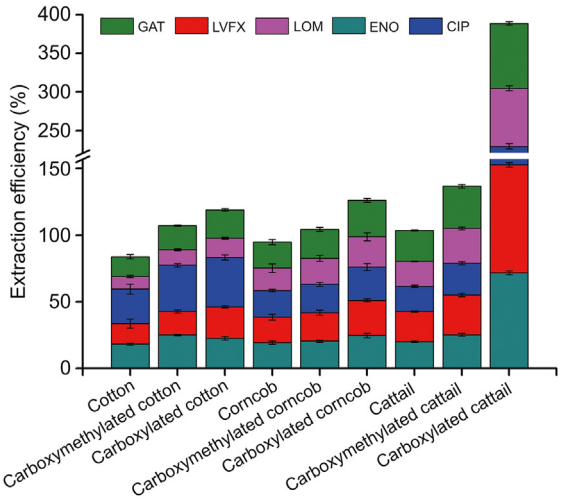

Fig. 4. Extraction performance of unmodified, carboxymethylated, and carboxylated cotton, cattail, and corncob for fluoroquinones. GAT: gatifloxacin; LOM: lomefloxacin hydrochloride; CIP: ciprofloxacin; LVFX: levofloxacin; ENO: enoxacin sesquihydrate.

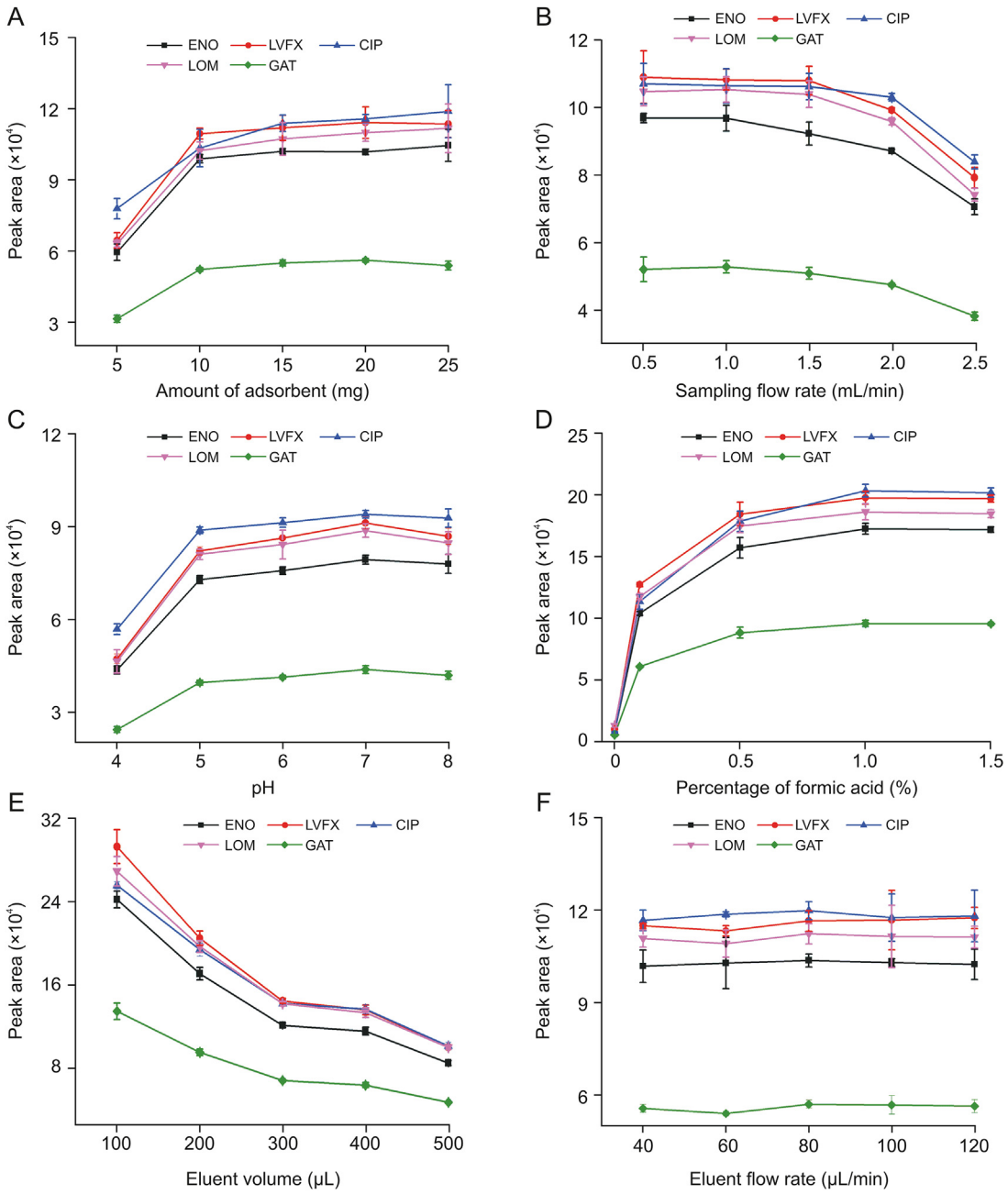

Fig. 5. Effect of the (A) adsorbent amount, (B) flow rate of the sample solution, (C) pH, (D) desorption solvent, (E) eluent volume, and (F) flow rate of the eluent on the extraction of fluoroquinones (FQs). ENO: enoxacin sesquihydrate; LVFX: levofloxacin; CIP: ciprofloxacin; LOM: lomefloxacin hydrochloride; GAT: gatifloxacin.

the carboxylated cattail and the analytes. Based on stronger hydrogen bonding, electrostatic interaction and Lewis acid-base interaction, most of the LVFX was adsorbed by carboxylated cattail. This indicated that carboxylated cattail was selective toward LVFX and other similar FQs.

3.4. Extraction and removal performance

The extraction and removal performances were evaluated using the EE (%) and adsorption amount (μg/g), respectively. The sampling solution (10 mL) with 40.5 μg/L ENO, 40 μg/L CIP, 49.5 μg/L LVFX, 54.6 μg/L LOM, and 41.4 μg/L GAT was loaded onto the micro-column under optimal extraction conditions to calculate EE. The EE was calculated from the ratio of the extraction amount to the initial amount. The EE was 71.5% for ENO, 78.3% for LVFX, 73.8% for CIP, 71.3% for LOM, and 80.9% for GAT. The hydrogen bonding (−N−H···O and −O−H···O), Lewis acid-base (PF−COOH to piperazine ring), and electrostatic interactions between FQs and carboxylated might lead to high EE. The unique structure of cattail and its high hemicellulose and lignin contents contributed to enhancing the hydrogen bonding and van der Waals interactions. The higher EE of LVFX and GAT could be attributed to the stronger hydrogen bonding effects caused by oxygenated heterocycles of LVFX and methoxy of GAT.

To investigate the breakthrough volume for FQs, the sample solution was loaded continuously and the outlet solution was collected for analysis. The adsorption amount was calculated using Eq. (2), which was based on the breakthrough curve (Fig. S4). The c_t increased as time progressed and was equal to c_0 until saturation.

The breakthrough time was about 5 min. The long exhaustion time was 162 min for ENO, 144 min for LVFX, 162 min for CIP, 156 min for LOM, and 138 min for GAT, demonstrating that the adsorbent exhibited rapid adsorption, followed by a slow balancing process for FQs. The adsorption amounts were 67.2 μg/g for ENO, 84.8 μg/g for LVFX, 45.8 μg/g for CIP, 97.6 μg/g for LOM, and 59.0 μg/g for GAT. The higher accumulated adsorption amount of LVFX and LOM could be because the two molecules preferentially occupied the adsorption sites on the carboxylated cattail. Although the saturation absorption of LVFX and LOM affected the adsorption amounts of the other FQs, the results indicated the potential for the simultaneous removal of five FQs using carboxylated cattail. Overall, the high EE and adsorption capacity demonstrated that carboxylated cattail was capable of successfully adsorbing FQs from aqueous solutions.

3.5. Reproducibility and reusability

The reproducibility of carboxylated cattail was performed to investigate the stability of the modification method. Under optimal extraction conditions, carboxylated cattail samples from the same batch and from seven batches were employed for the extraction of FQs ($n = 3$). The results suggested that good reproducibility was obtained with relative standard deviations (RSDs) of 2.9% for ENO, 3.7% for LVFX, 2.3% for CIP, 3.2% for LOM, and 3.4% for GAT in intra-batch, and RSDs of 6.6% for ENO, 5.9% for LVFX, 8.9% for CIP, 6.0% for LOM, 5.8% for GAT in inter-batch.

The reusability of the adsorbent was tested by performing the extraction of FQs over multiple usage cycles. After each round of extraction, 1 mL of aqueous ACN:1% formic acid (1:1, *V*/*V*) and 40 mL of ultrapure water were successively loaded through the cartridge at a flow rate of 100 μL/min and 1 mL/min, respectively, to remove the residual analytes. The results are presented in Fig. S5. Results showed that there was no obvious variation in the extracted amounts of FQs within 10 extraction cycles and had RSDs of 3.4% for ENO, 3.8% for LVFX, 3.2% for CIP, 4.2% for LOM, 3.6% for GAT. This indicated that the adsorbent had good reusability. The good reproducibility and reusability ensured the stability of carboxylated PFs in the preparation and application.

3.6. Analytical performance

The carboxylated cattail packed IS-SPE was used to analyze the trace FQs coupled with UPLC-PDA. To validate the analytical performance of the proposed method, the LOD and limit of quantification (LOQ), linear range, and repeatability were determined. Blank river water samples spiked with different concentrations of FQs were tested for the extraction of FQs and the results are in Table 1. The LODs based on signal to noise ratio (S/N) of 3 were within the range of 0.08–0.25 μg/L and LOQs (S/N = 10) were within the range of 0.26–1.00 μg/L. Satisfactory linearity was within the range of 0.5–100 μg/L with the correlation coefficient varying from 0.9992 to 0.9996. The repeatability was evaluated by three parallel extractions from samples containing 20 μg/L of FQs, and the RSDs were found to be within the range of 4.1%–5.7%. These results indicated that the developed method for the analysis of trace FQs possessed high sensitivity, good linearity, and repeatability.

To evaluate the extraction performance of the current method, the comparison with other reported methods is shown in Table 2 [1,4,9,19,47,48]. Compared to the methods employing restricted access media-molecularly imprinted nanomaterial [47], MIP [4], and hyper-crosslinked strong anion-exchange polymer resins [48], higher sensitivity and lower required amounts of adsorbent were achieved using the proposed method and the adsorbent. The sensitivity was slightly lower than that of the methods employing ILs/Fe_3O_4@Zr-MOFs [19] with high-resolution mass spectrometry detector, tris(4-aminophenyl)amine-tris(4-formylphenyl)benzene-COFs with mass spectrometry [1], and commercial polymer cation exchange material [9]. Interestingly, the green preparation method proposed in the current work is feasible and reproducible and boasts a solvent-free consumption. Therefore, the facile carboxylation of PFs is significant in the recycling of plant fibers waste.

Table 1
Analytical performance of IS-SPE-UPLC-PDA method to detect fluoroquinolones (FQs) in the river water.

Analytes	LOD (μg/L, S/N = 3)	LOQ (μg/L, S/N = 10)	Linear range (μg/L)	Correlation coefficient (R^2)	Calibration equation	RSD (%, $n = 3$, concentration: 20 μg/L)
ENO	0.08	0.26	0.5–100	0.9993	$y = (1125.2 \pm 28.6)x + 29.5 \pm 2.4$	4.1
OFL	0.15	0.50	0.5–100	0.9995	$y = (963.7 \pm 12.7)x + 199.7 \pm 17.2$	5.7
CIP	0.08	0.26	0.5–100	0.9992	$y = (1479.7 \pm 12.7)x + 280.6 \pm 17.1$	4.1
LOM	0.10	0.34	0.5–100	0.9996	$y = (842.2 \pm 3.8)x + 2045.2 \pm 69.5$	5.0
GAT	0.25	1.00	1.0–100	0.9994	$y = (441.3 \pm 4.7)x + 161.3 \pm 0.2$	5.7

IS-SPE-UPLC-PDA: in-syringe solid phase extraction-ultra-performance liquid chromatography-photodiode array detector; LOD: limit of detection; S/N: signal to noise ratio; LOQ: limit of quantitation; RSD: relative standard deviations; ENO: enoxacin sesquihydrate; OFL: ofloxacin; CIP: ciprofloxacin; LOM: lomefloxacin; GAT: gatifloxacin.

Table 2
A comparison between carboxylated cattail packed IS-SPE-UPLC-PDA and other reported methods for determination of FQs.

Method	Analyte	Adsorbent	Preparation method	Matrix	Adsorbent amount (mg)	LOD	Refs.
SPE-LC/MS/MS	CIP and GAT	TAPA-TFPB-COFs	Solvent synthesis	Water and meat	100	0.03–0.09 ng/L	[1]
SPE-HPLC-UV	CIP	MIP	Solvothermal method	Water	10	0.11 μg/L	[4]
DMSPE-LC-HRMS	CIP and OFL	PCX	Commercial adsorbent	Serum and urine	20	0.02–0.03 μg/L	[9]
MSPE-HPLC-DAD	OFL, CIP, and GAT	ILs/Fe_3O_4@Zr-MOFs	Solvothermal method	Water	5	0.02 μg/L	[19]
DSPE-HPLC-UV	OFL and GAT	RAM-MIPs	Solvothermal method	Milk and river water	20	0.93–1.31 μg/L	[47]
SPE-HPLC-UV	ENO, CIP, and LOM	HXLPP-SAX	Solvothermal method	Milk	60	2.80–3.90 ng/g	[48]
IS-SPE-UPLC-PDA	ENO, GAT, LVFX, CIP, and LOM	Carboxylated cattail	Hydrothermal method	River water	15	0.08–0.25 μg/L	This work

IS-SPE-UPLC-PDA: in-syringe solid phase extraction-ultra-performance liquid chromatography-photodiode array detector; LOD: limit of detection; DMSPE: dispersivemicro solid phase extraction; LC-HRMS: liquid chromatography-high resolution mass spectrometry; CIP: ciprofloxacin; OFL: ofloxacin; PCX: polymer cation exchange material; MSPE: magnetic solid-phase extraction; HPLC: high performance liquid chromatography; DAD: diode array detection; GAT: gatifloxacin; ILs: ionic liquid; MOFs: metal organic frameworks; SPE: solid phase extraction; LC-MS/MS: liquid chromatography tandem mass spectrometry; TAPA-TFPB-COFs: the COFs synthesized by tris(4-aminophenyl) amine (TAPA) and tris(4-formylphenyl)benzene (TFPB) as monomers; DSPE: dispersive solid phase extraction; UV: ultraviolet; RAM-MIPs: restricted access media-molecularly imprinted nanomaterials; ENO: enoxacin sesquihydrate; LOM: lomefloxacin; HXLPP-SAX: hypercrosslinked strong anion-exchange polymer resins; LVFX: levofloxacin.

Table 3
Spiked recoveries of fluoroquinolones (FQs) in the river water, wetland water, and pond water ($n = 3$).

Analytes	Spiked (μg/L)	River water		Wetland water		Pond water	
		Determined concentration (μg/L)	Recovery (%)	Determined concentration (μg/L)	Recovery (%)	Determined concentration (μg/L)	Recovery (%)
ENO	0	–	–	–	–	–	–
	5	5.6 ± 0.2	111.0	4.6 ± 0.1	92.8	4.2 ± 0.4	83.8
	40	42.5 ± 2.4	106.3	40.4 ± 1.5	101.1	37.1 ± 1.1	92.8
	80	84.2 ± 0.9	105.3	81.5 ± 2.9	101.8	81.5 ± 2.9	101.8
LVFX	0	–	–	–	–	–	–
	5	5.3 ± 0.2	105.3	5.2 ± 0.2	104.7	5.3 ± 0.2	105.1
	40	43.7 ± 2.7	109.2	41.1 ± 1.9	102.8	42.3 ± 1.2	105.8
	80	85.0 ± 1.1	106.2	81.7 ± 4.2	102.1	81.7 ± 4.2	102.1
CIP	0	–	–	–	–	–	–
	5	5.3 ± 0.1	105.0	4.5 ± 0.1	90.8	4.3 ± 0.3	85.0
	40	42.3 ± 2.3	105.7	40.0 ± 1.3	99.9	35.5 ± 0.7	88.9
	80	83.7 ± 0.7	104.7	81.2 ± 2.7	101.5	81.2 ± 2.7	101.5
LOM	0	–	–	–	–	–	–
	5	4.9 ± 0.2	98.5	4.8 ± 0.1	95.7	5.1 ± 0.01	102.7
	40	40.9 ± 3.1	102.2	40.7 ± 1.8	101.8	44.5 ± 2.5	111.3
	80	82.7 ± 2.1	103.4	80.0 ± 4.6	100.0	80.0 ± 4.6	100.0
GAT	0	–	–	–	–	–	–
	5	5.6 ± 0.3	111.7	4.5 ± 0.4	89.6	4.7 ± 0.3	94.7
	40	43.6 ± 2.5	108.9	40.5 ± 2.0	101.3	41.3 ± 1.1	103.1
	80	85.4 ± 0.6	106.8	81.1 ± 3.3	101.4	81.1 ± 3.3	101.4

ENO: enoxacin sesquihydrate; LVFX: levofloxacin; CIP: ciprofloxacin; LOM: lomefloxacin; GAT: gatifloxacin; –: not detected.

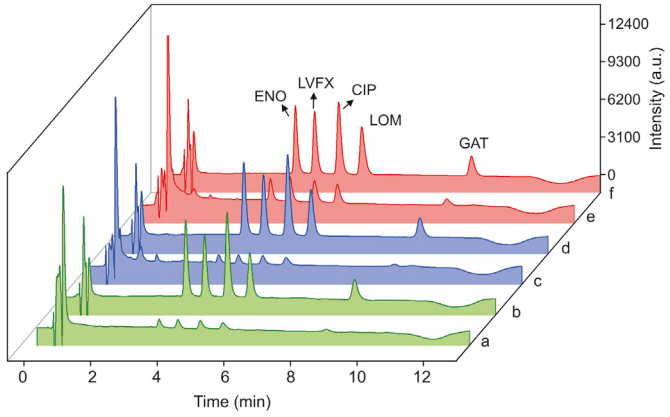

Fig. 6. Chromatograms of (a) river water, (c) wetland water, and (e) pond water spiked with 40 μg/L fluoroquinolones (FQs) before extraction. Chromatograms of (b) river water, (d) wetland water, and (f) pond water spiked with 40 μg/L FQs after extraction. ENO: enoxacin sesquihydrate; LVFX: levofloxacin; CIP: ciprofloxacin; LOM: lomefloxacin hydrochloride; GAT: gatifloxacin.

3.7. Application to real-life samples

The developed IS-SPE-UPLC-PDA method was performed to trace FQ residues in the natural water samples. No FQs were detected in the river water, wetland water, and pond water. The recoveries in the three water samples were determined by spiking 5, 40, and 80 μg/L of FQs to validate the accuracy of the developed method. As listed in Table 3, good recoveries were achieved lying within the range of 83.8%–111.7%. The typical chromatograms obtained are shown in Fig. 6. The FQ peaks significantly increased and no other compound was detected after the extraction. Therefore, the proposed method was accurate and reliable for the sensitive determination of FQs in natural water samples.

4. Conclusion

In the present work, carbohydrate-rich cotton, corncob, and cattail fibers were carboxylated using a simple hydrothermal reaction. The CA-modified carboxyl cattail exhibited the highest carboxyl content, which endowed the cattail fiber superior adsorption performance for the extraction of FQs from water samples. Strong hydrogen bonding, Lewis acid-base interactions, and electrostatic interactions acted as the main adsorption mechanisms. The preparation method was verified to be replicable and the prepared adsorbent was reusable in multiple adsorption cycles with RSDs ≤4.2%. Coupled with the detection of UPLC-PDA, the carboxylated cattail packed IS-SPE exhibited high sensitivity (0.08–0.25 μg/L), good repeatability (RSD ≤ 5.7%) and accuracy (83.8%–111.7% recovery) for the analysis of trace FQs in river water, wetland water, and pond water. The economical and green carboxyl-modified PFs can be applied to the adsorption of FQ antibiotics in water samples. Moreover, the modified corncob and cattail fibers used for the adsorption of drug pollutants have great significance in further recycling waste from biomass resources.

CRediT author statement

Nan Zhang: Investigation, Software, Writing - Original draft preparation; **Yan Gao:** Formal analysis, Visualization; **Kangjia Sheng:** Software, Validation; **Wanghui Jing:** Methodology; **Xianliang Xu:** Visualization; **Tao Bao:** Conceptualization, Methodology, Resources, Writing - Reviewing and Editing; **Sicen Wang:** Project administration, Writing - Reviewing and Editing, Funding acquisition, Supervision.

Declaration of competing interest

The authors declare that there are no conflicts of interest.

Acknowledgments

This work was supported by the National Natural Science Foundation of China (Grant Nos.: 81703469 and 81973277), Open Fund of the State Key Laboratory of Quality Research in Chinese Medicine, University of Macau (Grant No.: SKL-QRCM(UM)-2020-2022, QRCM-OP21007), and the World-Class Universities (Disciplines) and the Characteristic Development Guidance Funds for the Central Universities (Grant No.: PY3A012).

Appendix A. Supplementary data

Supplementary data to this article can be found online at https://doi.org/10.1016/j.jpha.2022.06.004.

References

[1] G. Xu, X. Dong, L. Hou, et al., Room-temperature synthesis of flower-shaped covalent organic frameworks for solid-phase extraction of quinolone antibiotics, Anal. Chim. Acta 1126 (2020) 82–90.
[2] K. Mogolodi Dimpe, P.N. Nomngongo, Application of activated carbon-decorated polyacrylonitrile nanofibers as an adsorbent in dispersive solid-phase extraction of fluoroquinolones from wastewater, J. Pharm. Anal. 9 (2019) 117–126.
[3] L. Fang, Y. Miao, D. Wei, et al., Efficient removal of norfloxacin in water using magnetic molecularly imprinted polymer, Chemosphere 262 (2021), 128032.
[4] G. Zhu, G. Cheng, P. Wang, et al., Water compatible imprinted polymer prepared in water for selective solid phase extraction and determination of ciprofloxacin in real samples, Talanta 200 (2019) 307–315.
[5] W. Shang, B. Qiao, Q.-M. Xu, et al., Potential biotransformation pathways and efficiencies of ciprofloxacin and norfloxacin by an activated sludge consortium, Sci. Total Environ. 785 (2021), 147379.
[6] W. Jiang, W.-R. Cui, R.-P. Liang, et al., Difunctional covalent organic framework hybrid material for synergistic adsorption and selective removal of fluoroquinolone antibiotics, J. Hazard Mater. 413 (2021), 125302.
[7] H. Yu, H. Mu, Y.-M. Hu, Determination of fluoroquinolones, sulfonamides, and tetracyclines multiresidues simultaneously in porcine tissue by MSPD and HPLC-DAD, J. Pharm. Anal. 2 (2012) 76–81.
[8] Y. Ma, P. Li, L. Yang, et al., Iron/zinc and phosphoric acid modified sludge biochar as an efficient adsorbent for fluoroquinolones antibiotics removal, Ecotoxicol. Environ. Saf. 196 (2020), 110550.
[9] R. Wang, S. Li, D. Chen, et al., Selective extraction and enhanced-sensitivity detection of fluoroquinolones in swine body fluids by liquid chromatography-high resolution mass spectrometry: Application in long-term monitoring in livestock, Food Chem. 341 (2021), 128269.
[10] A. Ashiq, M. Vithanage, B. Sarkar, et al., Carbon-based adsorbents for fluoroquinolone removal from water and wastewater: A critical review, Environ. Res. 197 (2021), 111091.
[11] Q. Zhang, Z. Zhu, X. Zhao, et al., Efficient and effective removal of emerging contaminants through the parallel coupling of rapid adsorption and photocatalytic degradation: A case study of fluoroquinolones, Chemosphere 280 (2021), 130770.
[12] Y. Gou, P. Chen, L. Yang, et al., Degradation of fluoroquinolones in homogeneous and heterogeneous photo-Fenton processes: A review, Chemosphere 270 (2021), 129481.
[13] X. Fang, S. Wu, Y. Wu, et al., High-efficiency adsorption of norfloxacin using octahedral UIO-66-NH_2 nanomaterials: Dynamics, thermodynamics, and mechanisms, Appl. Surf. Sci. 518 (2020), 146226.
[14] B. Gao, Q. Chang, J. Cai, et al., Removal of fluoroquinolone antibiotics using actinia-shaped lignin-based adsorbents: Role of the length and distribution of branched-chains, J. Hazard Mater. 403 (2021), 123603.
[15] X. Zhao, M. Zheng, X. Gao, et al., The application of MOFs-based materials for antibacterials adsorption, Coord. Chem. Rev. 440 (2021), 213970.
[16] W. Jiang, W.-R. Cui, R.-P. Liang, et al., Zwitterionic surface charge regulation in ionic covalent organic nanosheets: Synergistic adsorption of fluoroquinolone antibiotics, Chem. Eng. J. 417 (2021), 128034.
[17] A. Wen, G. Li, D. Wu, et al., Sulphonate functionalized covalent organic framework-based magnetic sorbent for effective solid phase extraction and determination of fluoroquinolones, J. Chromatogr. A 1612 (2020), 460651.
[18] H. Tian, T. Liu, G. Mu, et al., Rapid and sensitive determination of trace fluoroquinolone antibiotics in milk by molecularly imprinted polymer-coated stainless steel sheet electrospray ionization mass spectrometry, Talanta 219 (2020), 121282.
[19] D. Lu, M. Qin, C. Liu, et al., Ionic liquid-functionalized magnetic metal-organic framework nanocomposites for efficient extraction and sensitive detection of fluoroquinolone antibiotics in environmental water, ACS Appl. Mater. Interfaces 13 (2021) 5357–5367.
[20] F. Tan, D. Sun, J. Gao, et al., Preparation of molecularly imprinted polymer nanoparticles for selective removal of fluoroquinolone antibiotics in aqueous solution, J. Hazard Mater. 244–245 (2013) 750–757.
[21] N. Mohammed, N. Grishkewich, K.C. Tam, Cellulose nanomaterials: Promising sustainable nanomaterials for application in water/wastewater treatment processes, Environ. Sci. Nano 5 (2018) 623–658.
[22] D. Wang, A critical review of cellulose-based nanomaterials for water purification in industrial processes, Cellulose 26 (2019) 687–701.
[23] Y. Gao, S. Wang, N. Zhang, et al., Novel solid-phase extraction filter based on a zirconium meta-organic framework for determination of non-steroidal anti-inflammatory drugs residues, J. Chromatogr. A 1652 (2021), 462349.
[24] J. Liu, T.-W. Chen, Y.-L. Yang, et al., Removal of heavy metal ions and anionic dyes from aqueous solutions using amide-functionalized cellulose-based adsorbents, Carbohydr. Polym. 230 (2020), 115619.
[25] K. Dhali, M. Ghasemlou, F. Daver, et al., A review of nanocellulose as a new material towards environmental sustainability, Sci. Total Environ. 775 (2021), 145871.
[26] F. Rol, M.N. Belgacem, A. Gandini, et al., Recent advances in surface-modified cellulose nanofibrils, Prog. Polym. Sci. 88 (2019) 241–264.
[27] C. Li, H. Ma, S. Venkateswaran, et al., Sustainable carboxylated cellulose filters for efficient removal and recovery of lanthanum, Environ. Res. 188 (2020), 109685.
[28] H. Sehaqui, K. Kulasinski, N. Pfenninger, et al., Highly carboxylated cellulose nanofibers via succinic anhydride esterification of wheat fibers and facile mechanical disintegration, Biomacromolecules 18 (2017) 242–248.
[29] X. Xu, N. Zhang, Y. Gao, et al., MOF@COF functionalized cotton fiber as a platform for high performance extraction and removal of bisphenols from water samples, J. Environ. Chem. Eng. 10 (2022), 107072.
[30] M. Hashem, P. Hauser, B. Smith, Wrinkle recovery for cellulosic fabric by means of ionic crosslinking, Textil. Res. J. 73 (2003) 762–766.
[31] M. Liu, Z. Zhao, W. Yu, Comparative investigation on removal characteristics of tetracycline from water by modified wood membranes with different channel walls, Sci. Total Environ. 775 (2021), 145617.
[32] S. Wang, L. Wang, W. Kong, et al., Preparation, characterization of carboxylated bamboo fibers and their adsorption for lead(II) ions in aqueous solution, Cellulose 20 (2013) 2091–2100.
[33] F. Qin, Z. Fang, J. Zhou, et al., Efficient removal of Cu^{2+} in water by carboxymethylated cellulose nanofibrils: Performance and mechanism, Biomacromolecules 20 (2019) 4466–4475.
[34] J. Wang, M. Liu, C. Duan, et al., Preparation and characterization of cellulose-based adsorbent and its application in heavy metal ions removal, Carbohydr. Polym. 206 (2019) 837–843.
[35] H.S. Jhinjer, A. Singh, S. Bhattacharya, et al., Metal-organic frameworks functionalized smart textiles for adsorptive removal of hazardous aromatic pollutants from ambient air, J. Hazard Mater. 411 (2021), 125056.
[36] T. Bao, Y. Su, N. Zhang, et al., Hydrophilic carboxyl cotton for in situ growth of UiO-66 and its application as adsorbents, Ind. Eng. Chem. Res. 58 (2019) 20331–20339.
[37] A. Hu, G. Ren, J. Che, et al., Phosphate recovery with granular acid-activated neutralized red mud: Fixed-bed column performance and breakthrough curve modelling, J. Environ. Sci. (China) 90 (2020) 78–86.
[38] F. Cui, H. Li, C. Chen, et al., Cattail fibers as source of cellulose to prepare a novel type of composite aerogel adsorbent for the removal of enrofloxacin in wastewater, Int. J. Biol. Macromol. 191 (2021) 171–181.
[39] D. Rebaque, R. Martínez-Rubio, S. Fornalé, et al., Characterization of structural cell wall polysaccharides in cattail (*Typha latifolia*): Evaluation as potential biofuel feedstock, Carbohydr. Polym. 175 (2017) 679–688.
[40] C. Duan, X. Meng, C. Liu, et al., Carbohydrates-rich corncobs supported metal-organic frameworks as versatile biosorbents for dye removal and microbial inactivation, Carbohydr. Polym. 222 (2019), 115042.
[41] P. Satyamurthy, P. Jain, R.H. Balasubramanya, et al., Preparation and characterization of cellulose nanowhiskers from cotton fibres by controlled microbial hydrolysis, Carbohydr. Polym. 83 (2011) 122–129.
[42] D.D. Sewu, P. Boakye, S.H. Woo, Highly efficient adsorption of cationic dye by biochar produced with Korean cabbage waste, Bioresour. Technol. 224 (2017) 206–213.
[43] H. Lin, S. Han, Y. Dong, et al., The surface characteristics of hyperbranched polyamide modified corncob and its adsorption property for Cr(VI), Appl. Surf. Sci. 412 (2017) 152–159.
[44] L.K. Kian, M. Jawaid, H. Ariffin, et al., Isolation and characterization of nanocrystalline cellulose from roselle-derived microcrystalline cellulose, Int. J. Biol. Macromol. 114 (2018) 54–63.
[45] S. Naduparambath, T.V. Jinitha, V. Shaniba, et al., Isolation and characterisation of cellulose nanocrystals from sago seed shells, Carbohydr. Polym. 180 (2018) 13–20.
[46] Y. Yang, L. Zheng, T. Zhang, et al., Adsorption behavior and mechanism of sulfonamides on phosphonic chelating cellulose under different pH effects, Bioresour. Technol. 288 (2019), 121510.
[47] J. Li, Y. Zhou, Z. Sun, et al., Restricted access media-imprinted nanomaterials based on a metal-organic framework for highly selective extraction of fluoroquinolones in milk and river water, J. Chromatogr. A 1626 (2020), 461364.
[48] X. Liang, P. Hu, H. Zhang, et al., Hypercrosslinked strong anion-exchange polymers for selective extraction of fluoroquinolones in milk samples, J. Pharm. Biomed. Anal. 166 (2019) 379–386.